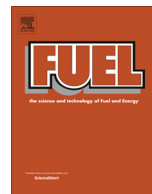




Contents lists available at ScienceDirect

Fuel

journal homepage: www.elsevier.com/locate/fuel

Full Length Article

Impact of coal matrix strains on the evolution of permeability

Yan Peng^{a,c}, Jishan Liu^{b,c,d,*}, Zhejun Pan^e, Luke D. Connell^e, Zhongwei Chen^f, Hongyan Qu^{b,g}^a College of Petroleum Engineering, China University of Petroleum (Beijing), 18 Fuxue Road, Changping, Beijing 102200, China^b State Key Laboratory of Geomechanics and Geotechnical Engineering, Institute of Rock and Soil Mechanics, Chinese Academy of Sciences, Hubei 430071, China^c School of Mechanical and Chemical Engineering, The University of Western Australia, 35 Stirling Highway, WA 6009, Australia^d IRC for Unconventional Geomechanics, Key Laboratory of Ministry of Education on Safe Mining of Deep Metal Mines, Northeastern University, Shenyang 110819, China^e CSIRO Energy, Private Bag 10, Clayton South 3169, Australia^f School of Mechanical and Mining Engineering, The University of Queensland, QLD 4072, Australia^g State Key Laboratory of Petroleum Resources and Prospecting, China University of Petroleum, 18 Fuxue Road, Changping, Beijing 102249, China

ARTICLE INFO

Article history:

Received 20 February 2016

Received in revised form 2 June 2016

Accepted 17 October 2016

Available online xxx

Keywords:

Coal permeability
Internal swelling
Gas adsorption
Matrix strain

ABSTRACT

The goal of this study is to investigate how coal matrix strains affect the evolution of coal permeability. In previous studies, this impact was quantified through splitting the matrix strain into two parts: one contributes to the internal swelling while the other to the global strain. It was assumed that the difference between the internal swelling strain and the swelling strain of matrix determines the evolution of fracture permeability through a constant splitting factor. This assumption means that the impact of internal swelling strain is always same during the whole gas injection/production process. This study extends this concept through the introduction of a strain splitting function that defines the heterogeneous distribution of internal swelling. The distribution function changes from zero to unity. Zero means that the internal swelling strain has no impact on permeability evolution while unity means 100% of the internal strain contributes to the evolution of coal permeability. Based on this approach, a new permeability model was constructed and a finite element model was built to fully couple the coal deformation and gas transport in coal seam reservoirs. The model was verified against three sets of experimental data under the condition of a constant confining pressure. Model results show that evolution of coal permeability under the condition of a constant confining pressure is primarily controlled by the internal strain at the early stage, by the global strain at the later stage, and by the strain splitting function in-between, and that the impact of the heterogeneous strain distribution on the internal swelling strain vanishes as the swelling capacity of matrix increases.

© 2016 Elsevier Ltd. All rights reserved.

1. Introduction

Coal permeability significantly affects coalbed methane (CBM) production and long-term storage of CO₂ in coal reservoirs. Coal permeability is sensitive to two factors: effective stress and sorption-induced strain. For CBM production, the reduction of gas pressure increases the effective stress which in return reduces the permeability [1,2]. Meanwhile, the reduction of gas pressure decreases sorption-induced strain which in return increases the permeability [3]. The behavior of coal permeability change depends on the net influence of these two competing mechanisms [4,5].

A broad variety of models have been developed to represent the effects of sorption-induced strain and effective stress on the dynamic evolution of coal permeability over the last few decades [6]. The coal permeability models with the effect of effective stress were firstly proposed [1,7,8], and then the effect of sorption-induced strain on coal permeability evolution was introduced into coal permeability models [9–12]. In the field, it is usually assumed that the coal seam reservoir is under the uniaxial strain condition. The permeability models dealing with the permeability evolution in the field consider the effect of the horizontal effective stress rather than the volumetric effective stress [2,4,12–14]. In laboratory, the condition on the samples is different from the in-situ condition. Many permeability models with different assumptions and empirical parameters were proposed to analyze the experimental data [8,15,16]. Based on the poroelasticity theory, Zhang et al. [17] developed a strain-based porosity model and a permeability model under variable stress conditions.

* Corresponding author at: School of Mechanical and Chemical Engineering, The University of Western Australia, 35 Stirling Highway, WA 6009, Australia.

E-mail address: jishan.liu@uwa.edu.au (J. Liu).

Nomenclature

A	constant for β (fraction)	α	biot coefficient (fraction)
E	Young's modulus of coal (GPa)	β	strain splitting function (fraction)
G	shear modulus of coal (GPa)	β_p	strain splitting function for production process (fraction)
K	bulk modulus of coal (GPa)	δ_i	index indicating whether internal strain is valid in i th matrix
K_f	bulk modulus of fracture (GPa)	ε	strain (fraction)
K_s	bulk modulus of matrix (GPa)	ε_{in}	internal swelling strain (fraction)
P_0	initial pressure (MPa)	ε_v	volumetric strain of coal (fraction)
P_{in}	injection pressure (MPa)	ε_s	gas adsorption-induced swelling strain of the whole coal (fraction)
P_L	Langmuir pressure constant (MPa)	ε_L	overall Langmuir strain constant for coal (fraction)
P_{con}	confining pressure (MPa)	ε_{LI}	Langmuir strain constant for region I (fraction)
P_c	pressure constant for β (MPa)	ε_{LII}	Langmuir strain constant for region II (fraction)
P_{Low}	constant for β_p (MPa)	ε_{Lm}	Langmuir strain constant of matrix (fraction)
P_a	atmosphere pressure (MPa)	$\bar{\varepsilon}_{Lm}$	average Langmuir strain constant for matrix (fraction)
P_w	Wellbore pressure (MPa)	ε_{fs}	gas adsorption-induced strain of fracture (fraction)
V_b	volume of coal bulk (m^3)	ε_{ms}	gas adsorption-induced strain of matrix (fraction)
V_f	fracture volume (m^3)	μ	viscosity (Pa s)
V_m	matrix volume (m^3)	μ_{CO_2}	CO ₂ Viscosity (Pa s)
V_L	Langmuir sorption capacity (m^3/kg)	μ_{CH_4}	CH ₄ Viscosity (Pa s)
b	fracture aperture (m)	ν	Poisson's ratio of coal (fraction)
b_0	initial fracture aperture (m)	ρ_c	coal density (kg/m^3)
c_f	compressibility (MPa^{-1})	σ_c	overburden pressure (MPa)
c_{fA}	compressibility of Anderson coal (MPa^{-1})	$\bar{\sigma}$	mean compressive stress (MPa)
c_{fG}	compressibility of Gilson coal (MPa^{-1})	ϕ_0	initial porosity for dry coals (percentage)
k_0	initial permeability of the dry coal (m^2)	ϕ_{m0}	initial matrix porosity (percentage)
k_f	fracture permeability (m^2)	ϕ_{0A}	initial porosity of Anderson coal (percentage)
k_{f0}	initial fracture permeability (m^2)	ϕ_{0G}	initial porosity of Gilson coal (percentage)
k_{m0}	initial matrix permeability (m^2)		
p	pressure (MPa)		

Greek symbols

In our recent review paper [18], it was concluded that current coal permeability models are unable to describe results from stress-controlled shrinkage/swelling laboratory tests [19–22]. It was suggested that the reason is that the impact of coal matrix-fracture interactions inside coals has not been taken into consideration. This impact could induce the internal swelling strain inside coal affecting permeability evolution [23]. The internal swelling strain was assumed as a portion of the free swelling strain of the whole coal [23,24]. This statement may be not always true. Other study illustrated that the internal swelling strain could be approximately 50 times larger than the swelling strain of coal bulk because of the low fracture porosity [25]. Currently, many models use a constant coefficient to account for the effect of internal swelling strain on permeability [23–26]. Although the characteristics of internal swelling strain were not fully studied, these models could match experimental data much better than traditional coal permeability models [23,26].

In order to investigate the evolution of internal swelling strain, a conceptual model comprised of a matrix and a fracture is usually used [27–31]. It was concluded that the internal swelling strain results from the gas transport between matrix and fracture [27]. The effects of temperature and boundary condition on the evolution of internal swelling strain were also investigated [28,29]. Based on those above studies, a dual porosity model with the effect of internal swelling strain due to gas transport between matrix and fracture was proposed [32]. All properties of the matrix in this model are homogeneous. In this ideal case, the internal swelling strain disappears when the equilibrium state between matrix and fracture is achieved [27–29]. This ideal case is different from the reality that a coal matrix contains several types of organic materials with different percentage. It was observed in laboratory

that the swelling strain is unevenly distributed inside coal matrices [33,34]. The distribution of organic materials inside coal matrices may significantly affect the distribution of internal swelling strain. Currently, the characteristics of internal swelling strain in coal matrices and how to consider the effect of heterogeneous distribution of internal swelling strain on the coal permeability have been rarely investigated.

In this paper, a conceptual geometry comprised of a fracture and a matrix including two regions with different minerals was first built to illustrate the effect of internal swelling strain on permeability. Secondly, a variable representing the effect of heterogeneous distribution of internal swelling strains on permeability was introduced into permeability model for a coal bulk. This variable was proposed based on some published experimental observations and our understanding about the internal swelling strain from the above conceptual geometry. Thirdly, this new model was testified through three sets of experimental data and then implemented into a numerical simulation model fully coupling the coal deformation and gas transport in coal seam reservoirs.

2. Effect of internal swelling strain on permeability evolution

In this section, a conceptual geometry representing the matrix-fracture system of coal was built to illustrate the obvious effect of internal swelling strain inside coal on permeability evolution. Then new models would be developed in the next section to consider the effect of internal swelling strain on permeability evolution. In this study, the adsorption-induced strain around fracture is called as the internal swelling strain. The matrix of coal as shown in Fig. 1 is divided into two regions with different adsorption capacities. This conceptual geometry is under the condition of free swelling

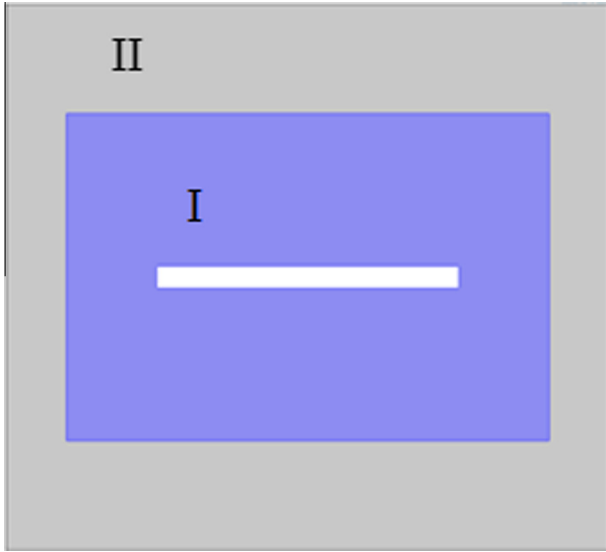


Fig. 1. Illustration of the conceptual geometry (The matrix block is divided into two regions with different adsorption capacities: region I and region II; the white rectangle represents the fracture).

as shown in Fig. 2. P_{con} and P_f are the confining pressure and fracture pressure, respectively. Initially, pressures in these two matrix regions and the fracture are the same. When the injection pressure is applied in the fracture, gas transports from the fracture into the matrix. The mass conservation of this transport process for ideal gas is [17]:

$$\left[\phi_i + \frac{\rho_c p_a V_{Li} P_{Li}}{(p_i + P_{Li})^2} \right] \frac{\partial p_i}{\partial t} + p_i \frac{\partial \phi_i}{\partial t} - \nabla \cdot \left(\frac{k_i}{\mu} p_i \nabla p_i \right) = 0 \quad (1)$$

where ϕ is the porosity, ρ_c is the coal density, p_a is the atmospheric pressure, V_L and P_L are two Langmuir constants, p is pressure, k is the permeability, μ is the viscosity, and the subscript i indicates the index of matrix regions. The adsorption-induced strains of these regions are subjected to the swelling strain, which is described using the Langmuir-like equation:

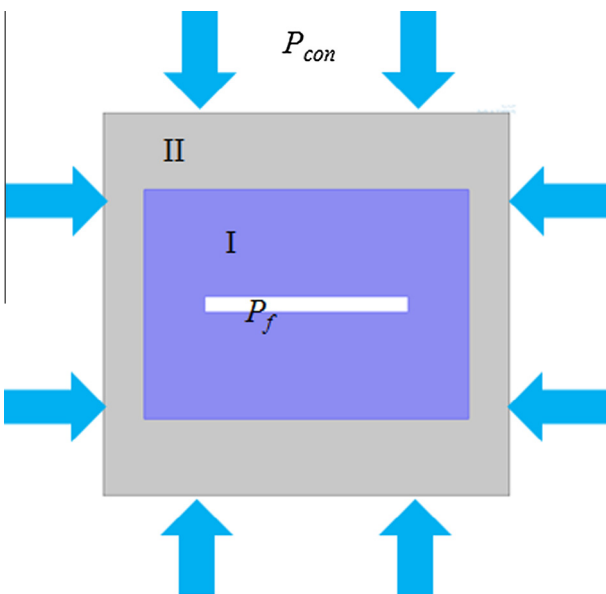


Fig. 2. Illustration of mechanical condition of the conceptual geometry.

Table 1
Input parameters of simulations.

Symbol	Value	Units
E	4	GPa
ν	0.3	–
α	0.66	–
μ	1.2×10^{-5}	Pa s
ϕ_{m0}	5	%
k_{m0}	1×10^{-20}	m^2
P_0	0.1	MPa
P_{in}	4	MPa
P_L	2	MPa
P_{con}	0	MPa
V_L	0.01316	m^3/kg
ρ_c	1500	kg/m^3
P_a	0.1	MPa
$b0$	0.4	mm

$$\varepsilon_s = \frac{\varepsilon_L p}{p + P_L} \quad (2)$$

where ε_s is the gas adsorption-induced strain, ε_L is the Langmuir strain constant, P_L is the Langmuir pressure constant for swelling strain. To simplify numerical simulations, it is assumed that the Langmuir pressure constants (P_L) of these two regions are the same but the Langmuir strain constants (ε_L) of these two regions are different. The Langmuir strain constants of different regions for three different scenarios are given in Table 2. All the values are selected within the range reported by Robertson and Christiansen [35].

Meantime, the fracture aperture changes with respect to pressure and this change can be calculated in the COMSOL model used in this work. The permeability of this conceptual geometry is calculated by the fracture aperture as shown in Eq. (3) [27]:

$$\frac{k_f}{k_{f0}} = \left(1 + \frac{\Delta b}{b_0} \right)^3 \quad (3)$$

where k_f is the fracture permeability and b is the fracture aperture. The subscript “0” represents the initial value of a parameter at the initial gas pressure (P_0) and the sign “ Δ ” represents the change between the current state and the initial state. Values of these parameters are selected from other studies [17,21,22,29,32] and listed in Table 1.

To illustrate the effect of internal swelling strain on permeability evolution, three simulation scenarios are studied in this work. In Scenario 1, there is no internal swelling strain (no adsorption-induced strain in region I) so the value of Langmuir strain constant in region I is set as 0. In Scenario 2, the internal swelling strain exists but there is no adsorption-induced strain in region II so the value of Langmuir strain constant in region II is set as 0. In Scenario 3, both the internal swelling strain and the adsorption-induced strain in region II exist but they have different values. The values of Langmuir strain constants in these two regions are set differently. In those three scenarios, except for the Langmuir strain constants, all other parameters and conditions are same. After the fracture aperture evolution with time is measured, the permeability evolution could be calculated by using Eq. (3).

In different scenarios, the swelling behaviors of these two regions are different. In Scenario 1, the swelling occurs only in region II far away from the fracture and the swelling strain does

Table 2
Langmuir strain constants of region I and region II for three scenarios.

	Scenario 1	Scenario 2	Scenario 3
ε_{LI}	0	0.03	0.01
ε_{LII}	0.03	0	0.03

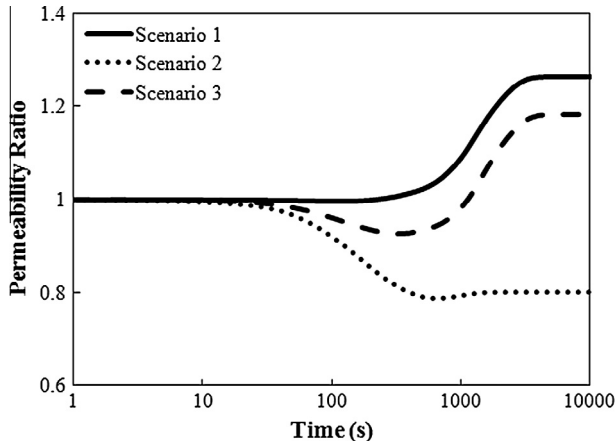


Fig. 3. Evolution of permeability ratio vs. time for different scenarios.

not exist in region I. The situation in Scenario 2 is totally opposite. These two scenarios are two extreme situations. The common situation is Scenario 3 where swelling occurs in both regions. The permeability of this conceptual geometry depends on the net change of swelling strains of region I and region II. The permeability ratio evolutions against time for different scenarios are illustrated in Fig. 3: For Scenario 1, the permeability always increases; for Scenario 2, the permeability always decreases. The difference in permeability evolution between these two scenarios discovers the effects of swelling strains in different regions on permeability. The swelling strain of the region far away from the fracture (region II) contributes to the volumetric strain of the coal bulk which increases the permeability. The swelling strain of the region around the fracture (region I) contributes to the internal swelling strain which decreases the permeability. For the common case like Scenario 3, swelling strains exist at both regions but dominate permeability evolution at different time. There is a transfer process existing. At first, the internal swelling strain dominates so the permeability decreases; afterwards, the volumetric swelling strain of the coal bulk dominates so the permeability increases. From this comparison, it is clear that the internal swelling strain results from the adsorption at matrix region around the fracture (region I as shown in Fig. 2) and also significantly affects permeability ratio at the equilibrium state. For different scenarios, the final values of permeability ratio are different even at the same pore pressure. It demonstrates that coal permeability evolution may depend on not only the pore pressure but also the internal swelling strain.

The conceptual geometry as shown in Fig. 1 represents only the simplest microscopic structure of coal with one fracture. In reality, the whole coal bulk as shown in Fig. 4 is comprised of a large number of such microscopic structures. Each microscopic structure has unique mineral components. The permeability of the whole coal bulk is the resultant of all swelling strains of these microscopic structures. In this case, the heterogeneity may also significantly affect permeability of the whole coal bulk.

3. Model formulation

From the above simple simulation, it is clear that the internal swelling strain and its distribution play important roles in permeability evolution. In this section, based on the above understanding and poroelasticity theory, the permeability model with the effects of the internal swelling strain and its distribution was developed. In addition, with considering the effect of distribution of internal swelling strain, the valid internal swelling strain that affects permeability evolution was proposed. Finally, to analyze the

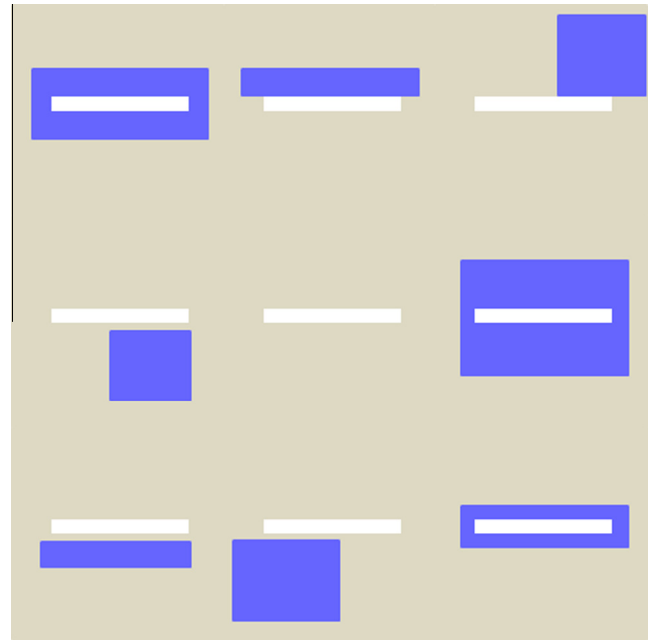


Fig. 4. Illustration of heterogeneity of microscopic structure of a coal bulk (The white rectangle represents the fracture; other components with different colors represents matrix regions with different minerals). (For interpretation of the references to colour in this figure legend, the reader is referred to the web version of this article.)

experimental data under the condition of constant confining pressure, the specific permeability model under the condition of constant confining pressure was generated.

3.1. General representation

In this section, the theoretical basis for the models developed in this paper was presented. First, on the basis of poroelasticity and by making an analogy between thermal contraction and sorption-induced swelling strain of the whole coal, the constitutive relation for the deformed coal is [17]:

$$\varepsilon_{ij} = \frac{1}{2G} \sigma_{ij} - \left(\frac{1}{6G} - \frac{1}{9K} \right) \sigma_{kk} \delta_{ij} + \frac{\alpha}{3K} p \delta_{ij} + \frac{\varepsilon_s}{3} \delta_{ij} \quad (4)$$

From the above equation, the volumetric strain of coal is:

$$\varepsilon_v = -\frac{1}{K} (\bar{\sigma} - \alpha p) + \varepsilon_s \quad (5)$$

where $\bar{\sigma} = -\sigma_{kk}/3$ is the mean compressive stress. G is the shear modulus of coal, E is the Young's modulus of coal, ν is the Poisson's ratio of coal, K is the bulk modulus of coal, α is the Biot coefficient, p is the pressure, and ε_s is the gas sorption-induced swelling strain of the whole coal.

Coal has fracture/cleat and matrix pore systems and is often simplified as a dual porosity reservoir [16]. It is commonly assumed that the fracture controls the flow and the pore in matrix controls the gas storage. In this paper, given the focus on gas flow, in the following, the calculation of porosity only considers the fractures rather than the pores in matrix. The volumetric balance between the volume of coal bulk (V_b), the matrix volume (V_m) and the fracture volume (V_f), is $V_b = V_m + V_f$. The porosity of coal (ϕ) is defined as: $\phi = V_f/V_b$. The differential volumetric strain of coal bulk (dV_b/V_b) and the differential volumetric strain of fractures (dV_f/V_f) can be expressed as: [17]:

$$\frac{dV_b}{V_b} = -\frac{1}{K} (d\bar{\sigma} - \alpha dp) + d\varepsilon_s \quad (6)$$

$$\frac{dV_f}{V_f} = -\frac{1}{K_f}(d\bar{\sigma} - \gamma dp) + d\varepsilon_s \quad (7)$$

where $\gamma = 1 - K_f/K_s$, K_f is the bulk modulus of fracture and K_s is the bulk modulus of matrix.

Based on the poroelasticity theory, the definition of porosity and the relationship between porosity and permeability, the ratio of current permeability to the initial permeability could be derived from the above two equations: [14,17]:

$$\frac{k}{k_0} = e^{-3c_f\Delta(\bar{\sigma}-p)} \quad (8)$$

According to the above equation, the permeability values should be the same if the confining pressure ($\bar{\sigma}$) and pore pressure (p) remain unchanged. However, it may not be true. In Fig. 3, at the equilibrium state (at around 10,000 s), the confining pressure and the pore pressure (equal to the injection pressure) are the same for different scenarios while their permeability values are different. The only difference between those three scenarios is the distribution of adsorption-induced swelling strain. If the internal swelling strain due to gas adsorption around fracture exists (Scenario 2 and Scenario 3), the permeability value will be less than that without the internal swelling strain (Scenario 1). According to Eq. (3), the alteration of fracture aperture has a close relationship with permeability. Since the permeability is affected by the internal swelling strain, the alteration of fracture volume is also affected by the internal swelling strain. The previous expression of the differential volumetric strain of fractures (Eq. (7)) already considers the adsorption-induced strain of the coal bulk (ε_s) but ignores the internal swelling strain. In order to consider the effect of the internal swelling strain on fracture volume, the differential volumetric strain of fracture (Eq. (7)) is modified as:

$$\frac{dV_f}{V_f} = -\frac{1}{K_f}(d\bar{\sigma} - \gamma dp) + d\varepsilon_s - d\varepsilon_{in} \quad (9)$$

where ε_{in} is the internal swelling strain. If the fracture is void as shown in Fig. 1, the matrix could deform freely towards fracture without any induced stress. If the internal swelling strain makes matrices contact each other, the internal force between matrices would be generated. The pair of internal force has equal values but opposite directions and the sum of this pair of internal force should be zero. In these two cases, the force balance of coal bulk (matrix-fracture system) is not changed. Thus the volumetric strain of coal bulk (Eqs. (5) and (6)) is not changed by the internal swelling strain inside coal bulk.

Using the definition of porosity, the following expression can be deduced [17]:

$$\frac{dV_b}{V_b} = \frac{dV_m}{V_m} + \frac{d\phi}{1-\phi} \quad (10)$$

$$\frac{dV_f}{V_f} = \frac{dV_m}{V_m} + \frac{d\phi}{(1-\phi)\phi} \quad (11)$$

Solving Eqs. (10) and (11), it yields:

$$\frac{d\phi}{\phi} = \frac{dV_f}{V_f} - \frac{dV_b}{V_b} \quad (12)$$

Substituting Eq. (6) and Eq. (9) into Eq. (12), it yields:

$$\frac{d\phi}{\phi} = \left(\frac{1}{K} - \frac{1}{K_f}\right)d(\bar{\sigma} - p) - d\varepsilon_{in} \quad (13)$$

As the bulk modulus K is commonly several orders of magnitude larger than the pore volume modulus, K_p , it is assumed that $\frac{1}{K} - \frac{1}{K_p} \approx -\frac{1}{K_p}$, then the compressibility can be defined as $c_f = \frac{1}{K_p}$. Therefore Eq. (13) becomes:

$$\frac{d\phi}{\phi} = -c_f d(\bar{\sigma} - p) - d\varepsilon_{in} \quad (14)$$

Integrating Eq. (14) gives:

$$\frac{\phi}{\phi_0} = e^{-c_f\Delta(\bar{\sigma}-p)-\Delta\varepsilon_{in}} \quad (15)$$

The typical relationship between porosity and permeability follows cubic law [18]:

$$\frac{k}{k_0} = \left(\frac{\phi}{\phi_0}\right)^3 \quad (16)$$

Substituting Eq. (15) into Eq. (16), the permeability model can be obtained:

$$\frac{k}{k_0} = e^{-3c_f\Delta(\bar{\sigma}-p)-3\Delta\varepsilon_{in}} \quad (17)$$

where ϕ_0 is the initial porosity, ϕ is the current porosity, k_0 is the initial permeability at initial pore pressure p_0 , k is the dynamic permeability at pore pressure p .

3.2. Derivation of the Internal Swelling Strain

When the coal is exposed to adsorptive gases such as CO_2 , the internal swelling strain inside the coal caused by gas adsorption as well as pressure increase is created [33]. The adsorption-induced strain is usually larger than the pressure-induced strain in coal. In this study, it is assumed that only the adsorption-induced strain contributes to the internal swelling strain;

A coal block is comprised of several maceral components with different percentage so there is a significant variation of adsorption-induced strains even at regional scales [36–38]. In this case, a matrix inside coal may have different adsorption properties from those of the whole coal. Applying a Langmuir-like equation, the adsorption-induced strain of a matrix inside coal is:

$$\varepsilon_{ms} = \frac{\varepsilon_{Lm}p}{p + P_{Lm}} \quad (18)$$

where ε_{ms} is the gas adsorption-induced strain of a matrix, ε_{Lm} is the Langmuir strain constant of a matrix and P_{Lm} is the Langmuir pressure constant of matrix strain. To simplify calculation, it is assumed that $P_{Lm} = P_L$ in this study, the relationship between adsorption-induced strain of a matrix and that of the whole coal bulk (Eq. (2)) is:

$$\varepsilon_{ms} = \frac{\varepsilon_{Lm}}{\varepsilon_L} \varepsilon_s \quad (19)$$

It is assumed that the matrix and fracture are always contacted. In this case, the fracture has the same volumetric change with the matrix. However, the sizes of fracture and matrix are much different. With the same volumetric change, their adsorption-induced strains are different. The volumetric change of matrix caused by gas adsorption is:

$$\Delta V_m = \varepsilon_{ms} V_{m0} \quad (20)$$

It should be equal to the volumetric change of fracture ($\Delta V_m = \Delta V_f$). In reality, the initial matrix volume is much larger than that of fracture ($V_{m0} \gg V_{f0}$) and the volume of coal bulk is the sum of volumes of matrix and fracture ($V_{b0} = V_{m0} + V_{f0}$). So the fracture strain caused by the volumetric change of matrix (Eq. (20)) is:

$$\varepsilon_{fs} = \frac{\Delta V_f}{V_{f0}} = \frac{\Delta V_m}{V_{f0}} = \varepsilon_{ms} \frac{V_{m0}}{V_{f0}} \approx \varepsilon_{ms} \frac{V_{m0} + V_{f0}}{V_{f0}} = \varepsilon_{ms} \frac{V_{b0}}{V_{f0}} = \frac{\varepsilon_{ms}}{\phi_0} \quad (21)$$

Substituting Eq. (19) into Eq. (21), the fracture strain becomes:

$$\varepsilon_{fs} = \frac{\varepsilon_{Lm}}{\varepsilon_L} \frac{1}{\phi_0} \varepsilon_s \quad (22)$$

The above equation is valid for an ideal case where the coal bulk has only a single matrix and a single fracture. The whole coal bulk includes a large number of matrices and fractures as shown in Fig. 4. Each matrix has unique adsorption capacity. Matrices with different strains may have interactions, which lead to the spatially heterogeneous distribution of matrix and fracture strains. Permeability evolution depends on the resultant of all these fracture strains. In this case, the valid internal swelling strain that changes the permeability is the average of all the valid fracture strains due to the adsorption-induced strains of matrix inside coal:

$$\varepsilon_{in} = \frac{1}{n} \sum_{i=1}^n \varepsilon_{fsi} \delta_i \quad (23)$$

where δ_i is the index indicating whether the fracture strain due to the adsorption-induced strains of matrix is valid in the i th matrix-fracture system. Its expression is defined as:

$$\delta_i = \begin{cases} 1, & \text{fracture strain valid} \\ 0, & \text{fracture strain invalid} \end{cases} \quad (24)$$

δ_i depends on where gas adsorption occurs. As discussion in Section 2, if the swelling only occurs at the matrix region far away from the fracture, the permeability always increases and is not affected by the internal swelling strain. It indicates that the impact of fracture strain is invalid for the internal swelling strain. If the swelling occurs at the matrix region around the fracture, the permeability always increases and is affected by the internal swelling strain. It indicates that the impact of fracture strain is valid for the internal swelling strain. Due to the heterogeneity in mineral components of a coal, any possibility of states of the fracture strain could coexist in coal.

Substituting Eq. (22) into Eq. (23), the internal swelling strain becomes:

$$\varepsilon_{in} = \frac{1}{n} \sum_{i=1}^n \frac{\varepsilon_{Lmi}}{\varepsilon_L} \frac{1}{\phi_0} \varepsilon_s \delta_i = \sum_{i=1}^n \frac{\varepsilon_{Lmi}}{n \varepsilon_L} \frac{1}{\phi_0} \varepsilon_s \delta_i \quad (25)$$

Because ε_L , ε_s , and initial porosity are the same for all matrices, they could be moved out from the summation sign, \sum , and Eq. (25) becomes:

$$\varepsilon_{in} = \frac{1}{\varepsilon_L \phi_0} \varepsilon_s \sum_{i=1}^n \frac{\varepsilon_{Lmi}}{n} \delta_i = \frac{\bar{\varepsilon}_{Lm}}{\varepsilon_L \phi_0} \varepsilon_s \sum_{i=1}^n \frac{\varepsilon_{Lmi}}{n \bar{\varepsilon}_{Lm}} \delta_i \quad (26)$$

where i is the index of the matrix number, n is the total number of matrices in coal, ε_{Lmi} is the Langmuir strain constant of i th matrix,

$\bar{\varepsilon}_{Lm}$ is the average of Langmuir strain constant of all matrices. For calculation convenience, in this study, a variable, β , is used to represent the heterogeneous distribution of valid internal swelling strain inside coal:

$$\varepsilon_{in} = \frac{\bar{\varepsilon}_{Lm}}{\varepsilon_L \phi_0} \varepsilon_s \sum_{i=1}^n \frac{\varepsilon_{Lmi}}{n \bar{\varepsilon}_{Lm}} \delta_i = \frac{\bar{\varepsilon}_{Lm}}{\varepsilon_L \phi_0} \varepsilon_s \beta \quad (27)$$

$$\beta = \sum_{i=1}^n \frac{\varepsilon_{Lmi}}{n \bar{\varepsilon}_{Lm}} \delta_i \quad (28)$$

where the range of β is from 0 to 1.

In addition, the heterogeneous distribution of valid internal swelling strain (β) may change with pore pressure. For example, as shown in Fig. 5, initially, the fracture is open and contributes to the permeability. In this case, the fracture strain of this matrix-fracture system affects permeability evolution so the validity of fracture strain (δ_i) is 1. If the fracture is closed due to the pore pressure change as shown in Fig. 5, this flow channel will stop to contribute to the permeability. In this case, the fracture strain of this matrix-fracture system will not affect permeability evolution so the validity of fracture strain (δ_i) is switched from 1 to 0. According to the definition of β (Eq. (28)), the alteration of δ_i changes β .

Some experimental observations [33,39,40] also imply that the heterogeneous distribution of internal swelling strain (β) depends on pore pressure. Although the effective stress is constant, it was observed that the distribution of internal swelling strain changes with pore pressure: with increase of pore pressure, the internal swelling strain at some locations increases while it decreases at other locations [33]. It was also observed that the distribution of gas adsorption in coal changes with pore pressure [39,40]. Because the internal swelling results from gas adsorption, it may be reasonable that the heterogeneous distribution of internal swelling strain (β) changes with pore pressure.

In this study, β is called as strain splitting function and its range is from 1 to 0. 0 means that the internal swelling strain has no impact on permeability evolution. 1 means that all the internal swelling strains inside coal affect permeability evolution. In order to reflect the fact that the distribution of internal swelling strain results from the gas adsorption described by the Langmuir theory, the second term of the β expression is assumed using the Langmuir-like equation:

$$\beta = 1 - A \frac{p - P_0}{P_c + p - P_0} \quad (29)$$

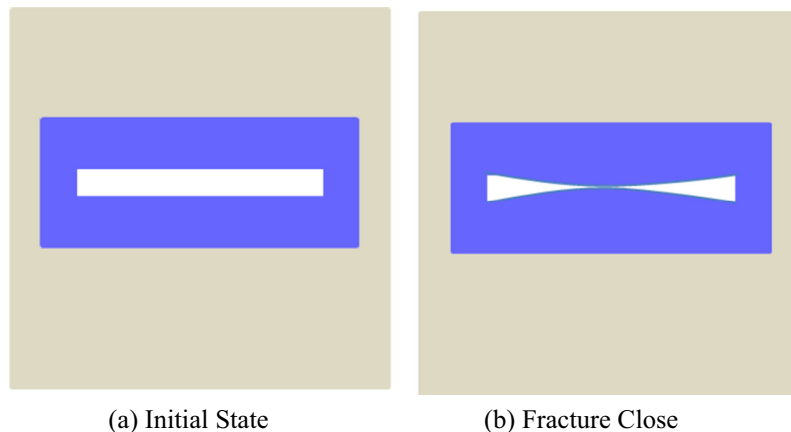


Fig. 5. Illustration of the change of microscopic structure inside a coal bulk (White part represents the fracture; areas with different colors represents different regions of matrix).

where A is a constant and represents the decrease rate of β . P_c is a constant which relates to confining pressure. Currently, the internal swelling strain is hard to be measured in laboratory and calculated in simulation models. In this study, with the introduction of β , the change of internal swelling strain inside coal (ε_{in}) could be calculated from the adsorption-induced strain of the whole coal bulk (ε_s):

$$\Delta\varepsilon_{in} = \beta C \Delta\varepsilon_s \quad (30)$$

where $C = \frac{\bar{\varepsilon}_{Lm}}{\varepsilon_L \phi_0}$ and it is a constant. It is an empirical equation but reflects some important mechanisms: (1) the internal swelling strain results from gas adsorption; (2) the impact of internal swelling strain on permeability is pressure-dependent.

Substituting Eq. (30) into Eq. (17), the evolution of permeability ratio is:

$$\frac{k}{k_0} = e^{-3c_f \Delta(\bar{\sigma}-p) - 3\beta C \Delta\varepsilon_s} \quad (31)$$

Substituting Eq. (5) into Eq. (31), the strain-based form of permeability evolution is:

$$\frac{k}{k_0} = e^{3c_f K (\Delta\varepsilon_v + \frac{\Delta p}{K_s} - \Delta\varepsilon_s) - 3\beta C \Delta\varepsilon_s} \quad (32)$$

3.3. Model arrangement for constant confining stress condition

In laboratory, the common condition applied at samples is the condition of constant confining pressure. In this case, the change of confining pressure ($\Delta\bar{\sigma}$) is zero. According to Eq. (31), the evolution of coal permeability under the condition of constant confining stress is:

$$\frac{k}{k_0} = e^{3c_f \Delta p - 3\beta C \Delta\varepsilon_s} \quad (33)$$

where the first term represents the impact of stress and the second term represents the impact of internal swelling strain on permeability evolution. It includes two main factors: (1) the heterogeneous distribution of internal strain (represented by β) and, (2) the difference between average adsorption-induced strain of matrices and adsorption-induced strain of the whole coal (represented by C). From this model, it is obvious that permeability not only depends on stress and adsorption-induced of coal bulk but also on the evolution of internal swelling strain of coal.

This model could explain some special observations. Under the condition of constant confining pressure, it was observed that permeability could decrease with pore pressure [21,22,35]. From the traditional model (Eq. (7)), the permeability should increase with pore pressure and this experimental phenomenon could not be explained. According to the new model (Eq. (33)), this special phenomenon is resulted from the internal swelling strain. The performance of our new model in matching experimental data is shown in Section 4.

3.4. Envelope of permeability evolution

Liu et al. [27] suggested an envelope of permeability evolution. This envelope defines the area which the permeability evolution under any condition should fall in. Its two bounds refer to two extreme situations. The first one is free swelling case where the confining pressure is constant ($\Delta\bar{\sigma} = 0$) and the effect of internal swelling strain on permeability evolution disappears ($\beta = 0$). Substituting these two constraints into Eq. (31), the first bound of the envelope is:

$$\frac{k}{k_0} = e^{3c_f \Delta p} \quad (34)$$

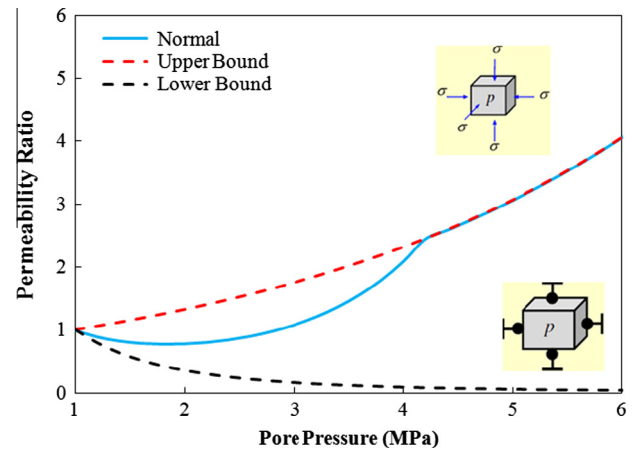


Fig. 6. Illustration of relationship of new model with two extreme cases.

Table 3
Input parameters.

Symbol	Value	Units
E	1.3	GPa
ν	0.3	-
α	0.6	-
ϕ_0	0.3	%
k_0	1.7×10^{-19}	m^2
P_0	1	MPa
P_L	6	MPa
ε_L	0.01	-
$\bar{\varepsilon}_{Lm}$	0.025	-
A	6	-
P_c	16	MPa

The other extreme situation is the constant volume where the volumetric change of coal is zero ($\Delta\varepsilon_v = 0$) and all the adsorbed gas contribute to the internal swelling strain ($\beta = 1$). Substituting these two constraints into Eq. (32), the other bound of the envelope is:

$$\frac{k}{k_0} = e^{3c_f K (\frac{\Delta p}{K_s} - \Delta\varepsilon_s) - 3C \Delta\varepsilon_s} \quad (35)$$

The model proposed in this study considers the effect of heterogeneous distribution of internal swelling strain on permeability evolution. Its relationship with these two extreme situations is illustrated in Fig. 6. The input parameters are collected from literature [19,32] and listed in Table 3. At first, the permeability evolution obtained from our model behaves like the one under the condition of constant volume, and then it behaves like the one under the condition of free swelling. It is consistent with majority of experimental observations [19,21,22]. In the following section, this new model is testified by experimental data and the evolution of β is analyzed.

4. Model validation against experimental data

In this section, the new model proposed in this study was validated by experimental data collected from Wang et al. [21], Vishal et al. [22] and Robertson and Christiansen [35]. These experiments were conducted under the condition of constant confining pressure. In this condition, the arrangement of our new model is Eq. (33). Meanwhile, the envelope of permeability evolution is also calculated by Eqs. (34) and (35). The input parameters are listed in Tables 4–9 for different literature data. The fracture porosity in coal could be as low as 0.28% [22]. In this study, it is assumed as 0.5% in Wang’s experiments and as 0.67% in Vishal’s experiments.

Table 4
Properties of coal for the experiment conducted by Wang et al. [21].

Symbol	Value	Units
ϕ	0.5	%
E	4.23	Gpa
c_f	0.2	MPa ⁻¹
α	0.6	–
ν	0.237	–

Table 5
Parameters used in matching the permeability obtained by Wang et al. [21].

Fluid	Confining Pressure	Symbol	Value	Units
CH ₄	6 MPa	k_0	1.7×10^{-19}	m ²
		P_0	1.7	MPa
		P_L	8	MPa
		ε_L	0.01	–
		$\bar{\varepsilon}_{Lm}$	0.048	–
		A	5	–
		P_c	14	MPa
CH ₄	12 MPa	k_0	1.53×10^{-20}	m ²
		P_0	1.7	MPa
		P_L	8	MPa
		ε_L	0.0027	–
		$\bar{\varepsilon}_{Lm}$	0.021	–
		A	4	–
		P_c	26	MPa
CO ₂	6 MPa	k_0	1.38×10^{-19}	m ²
		P_0	1.5	MPa
		P_L	8	MPa
		ε_L	0.016	–
		$\bar{\varepsilon}_{Lm}$	0.05	–
		A	4.5	–
		P_c	14	MPa
CH ₄	12 MPa	k_0	4.93×10^{-21}	m ²
		P_0	1.2	MPa
		P_L	8	MPa
		ε_L	0.013	–
		$\bar{\varepsilon}_{Lm}$	0.058	–
		A	6.5	–
		P_c	26	MPa

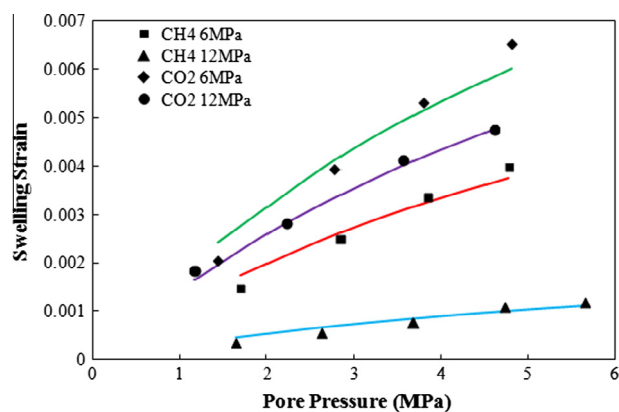
Table 6
Properties of coal and fluid for the experiment conducted by Vishal et al. [22].

Symbol	Value	Units
ϕ_0	0.67	%
E	4.23	Gpa
c_f	0.22	MPa ⁻¹
α	0.6	–
ν	0.237	–
P_0	1	MPa
P_L	8	MPa
ε_L	0.01	–

The Langmuir constants of adsorption-induced strain of the whole coal are obtained by matching the experimental data from Wang et al. [21]. The comparison of experimental data with results calculated by Langmuir equation (Eq. (2)) is illustrated in Fig. 7. Due to lack of data on adsorption-induced strain in the paper by Vishal et al. [22], the corresponding parameters are assumed as the same as the ones in experiments conducted by Wang et al. [21]. The Young's Modulus and Poisson's Ratio are collected from paper by Vishal et al. [22]. The value of compressibility is selected from the range from 0.194 to 0.485 MPa⁻¹ [41]. Those parameters for the experiments conducted by Robertson and Christiansen could be collected directly from their paper [35] and are listed in Tables 8 and 9. The values of A and $\bar{\varepsilon}_{Lm}$ are adjusted by matching

Table 7
Parameters used in matching the permeability obtained by Vishal et al. [22].

Confining pressure	Symbol	Value	Units
5 MPa	k_0	3.09×10^{-17}	m ²
	$\bar{\varepsilon}_{Lm}$	0.038	–
	A	2	–
	P_c	12	MPa
7 MPa	k_0	1.48×10^{-17}	m ²
	$\bar{\varepsilon}_{Lm}$	0.037	–
	A	1.6	–
	P_c	16	MPa
9 MPa	k_0	6.26×10^{-18}	m ²
	$\bar{\varepsilon}_{Lm}$	0.037	–
	A	1.6	–
	P_c	20	MPa
11 MPa	k_0	2.52×10^{-18}	m ²
	$\bar{\varepsilon}_{Lm}$	0.025	–
	A	0.7	–
	P_c	24	MPa
13 MPa	k_0	9.65×10^{-20}	m ²
	$\bar{\varepsilon}_{Lm}$	0.07	–
	A	14	–
	P_c	28	MPa

**Fig. 7.** Illustration of matching experimental data of adsorption-induced strain of the whole coal sample (dots are experimental data; lines are results calculated by Langmuir Equation).

experimental data. The values of P_c is determined by confining pressure and the relationship is $P_c = 2\sigma_c + 2$. The comparison of this model with experimental data are illustrated in Figs. 8–10.

In Figs. 8–10, the matching results are shown as solid lines, the experimental data are shown as dots, and the two bounds of permeability evolution are shown as dashed lines and the evolution of β is shown as the dotted line. All the experimental data should not exceed the two bounds. The new model proposed in this study matches experimental data very well because it considers the dynamic impact of internal swelling strain on permeability evolution. When the impact of internal swelling strain is large enough, the permeability ratio under the condition of constant confining pressure will decrease like the one under the condition of constant volume. With the decrease in the impact of internal swelling strain, the permeability ratio will recover and will increase like its ideal solution that excludes the impact of internal swelling strain. All the experiments conducted by Wang et al. [21] and Robertson and Christiansen [35] experienced this process: permeability decrease at low pore pressure and increase at high pore pressure as shown in Figs. 8 and 10. If the impact of internal swelling strain does not decrease enough, the permeability ratio will not recover. Majority of experiments conducted by Vishal et al. [22] did not

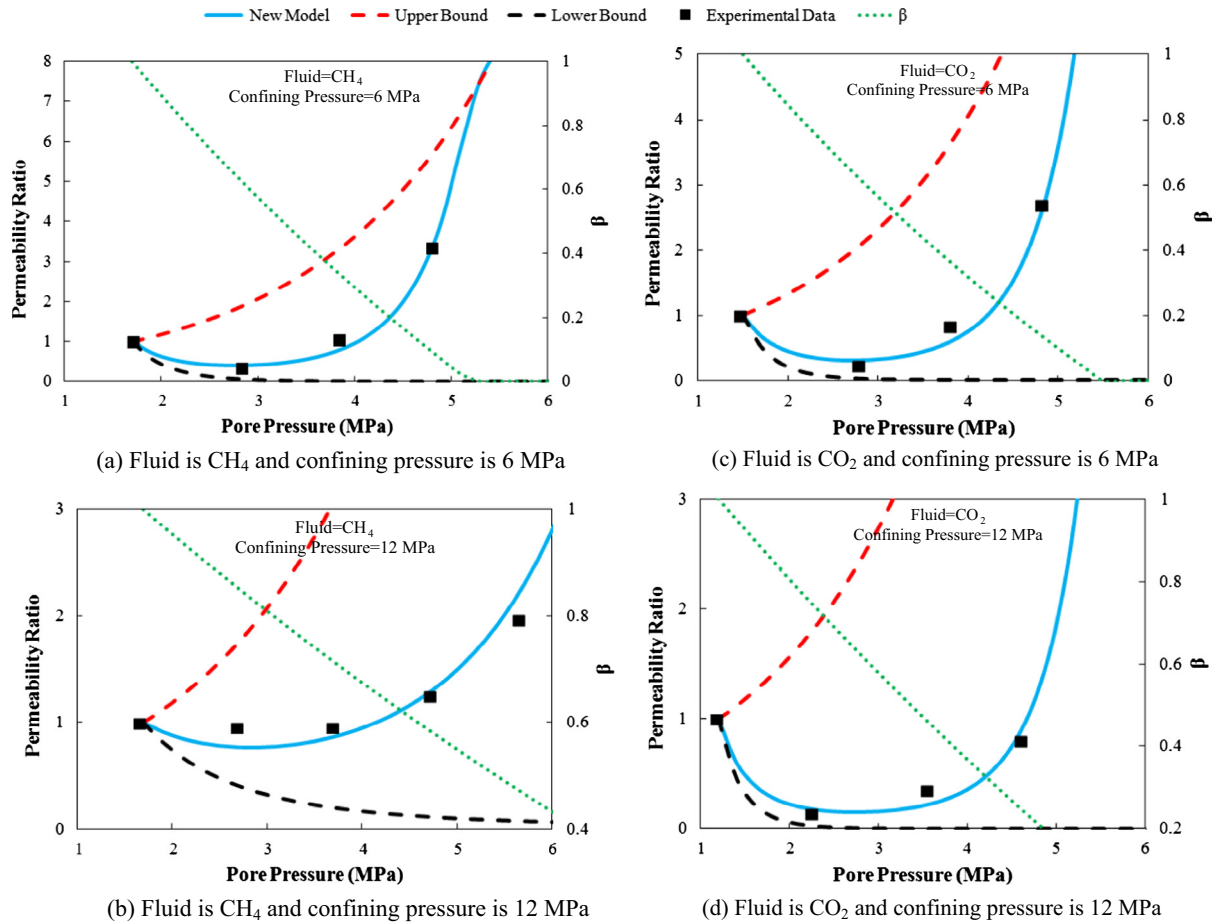


Fig. 8. Comparison of new model with experimental data obtained by Wang et al. [21], evolution of β and envelope of coal permeability evolution.

experience the recovery process as shown in Fig. 9. If the dynamic impact of internal swelling strain is considered, the complex behavior of permeability evolution could be explained and matched.

The evolution of β also shows in Figs. 8–10. In this study, β is determined by two parameters: A and P_c . The parameter A represents the decrease rate of β with pore pressure and P_c represents the impact of confining pressure. For majority of experimental observations, the profiles of permeability evolution for the same gas under different confining pressures are quite different. The increase of permeability is easily observed under high confining pressure. Based on this phenomenon, the impact of confining pressure on β was considered in this model. Currently, due to the lack of corresponding investigation, in this study, the relationship of P_c with confining pressure (σ_c) is only assumed as $P_c = 2\sigma_c + 2$. A is adjusted by matching experimental data. It is found that A increases with $\bar{\varepsilon}_{Lm}$ as shown in Fig. 11. It means that if the matrix inside coal has a higher adsorption-induced swelling ratio, the impact of internal swelling strain on permeability (β) decreases faster with pore pressure.

5. Application to coal seam gas reservoirs

In this section, the application of the new permeability model to coal seam gas reservoirs was illustrated. The simulation model includes two governing equations which represent mechanical deformation of coal seams and gas flow in coal seams, respectively. The new permeability model is used to be coupled with those two governing equations.

5.1. Governing equation of the mechanical deformation of coal

On the basis of poroelasticity and by making an analogy between thermal contraction and coal swelling, the equation of motion for the coal is [17]:

$$Gu_{i,kk} + \frac{G}{1-2\nu}u_{k,ki} - \alpha p_{,i} - K\varepsilon_{s,i} + f_i = 0 \quad (36)$$

where G is the shear modulus of coal, E is the Young's modulus of coal, ν is the Poisson's ratio of coal, K_s is the bulk modulus of matrix, α is the Biot coefficient, p is the gas pressure, ε_s is the gas adsorption-induced strain of coal and subject to Eq. (17), and f is the body force of coal, u is the displacement of coal.

5.2. Governing equation of the gas flow in coal

The gas mass in the fractured coal exists in both free-phase and adsorbed-phase forms. Applying the mass conservation law and Darcy velocity to the gas gives [17]:

$$\left[\phi + \frac{\rho_c p_a V_L P_L}{(P_L + p)^2} \right] \frac{\partial p}{\partial t} + p \frac{\partial \phi}{\partial t} - \nabla \cdot \left(\frac{k}{\mu} p \nabla p \right) = Q_s \quad (37)$$

where ϕ is the current porosity, k is the dynamic permeability, ρ_c is coal density, p_a is the atmosphere pressure, V_L and P_L are two Langmuir constants, p is reservoir pressure, μ is the viscosity and Q_s is the source.

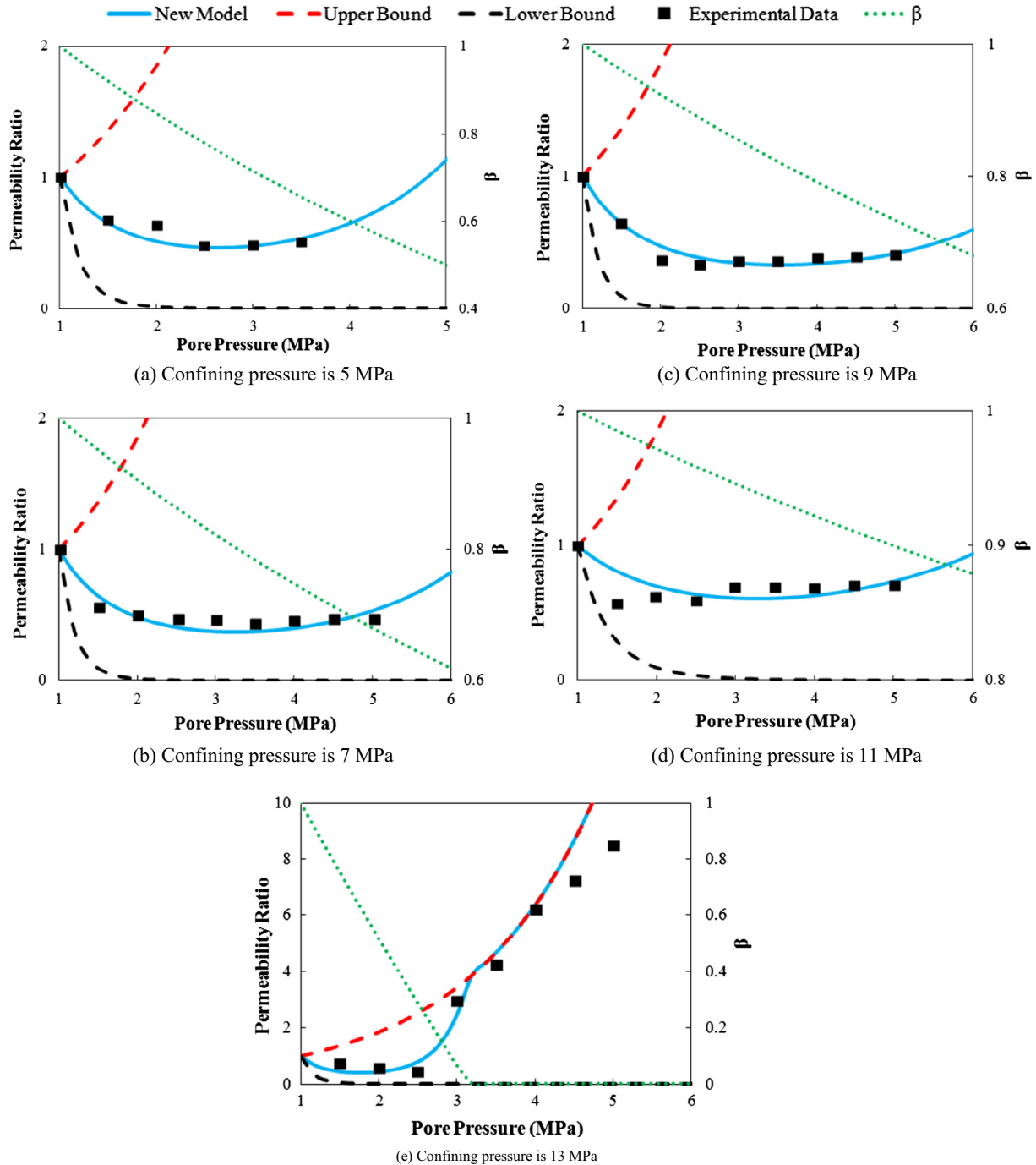


Fig. 9. Comparison of new model with experimental data obtained by Vishal et al. [22], evolution of β and envelope of coal permeability evolution.

5.3. Permeability model

The permeability model is the same as Eq. (32). However, this model was proposed based on the gas injection process. When it is used to a production process, the strain splitting function (β) should be slightly modified as:

$$\beta_p = 1 - A \frac{p - P_{Low}}{P_c + p - P_{Low}} \quad (38)$$

where β_p represents the strain splitting function (β) for production process and, P_{Low} represents the pressure where β_p reaches at 1. The only different between Eqs. (38) and (29) is that P_0 is displaced by P_{Low} . This change is made based on the characteristics of β . At low pressure, β is significant and decreases with pore pressure. During

the gas injection process, the lowest pressure is the initial pressure so the expression of β (Eq. (29)) involves P_0 . However, during the gas production process, the initial reservoir pressure is the highest pressure. According to the characteristics of β , β for production process should be the lowest at the initial reservoir pressure (P_0). In order to make the evolution of β for production process obey the characteristics of β , the expression of β for production process is changed as Eq. (38).

5.4. Model setting

In Fig. 12, the geometry represents a quarter of coal seam gas reservoir. The reservoir is a square with 50 m-length and the well with 5 cm radius locates at the bottom left. The boundary condi-

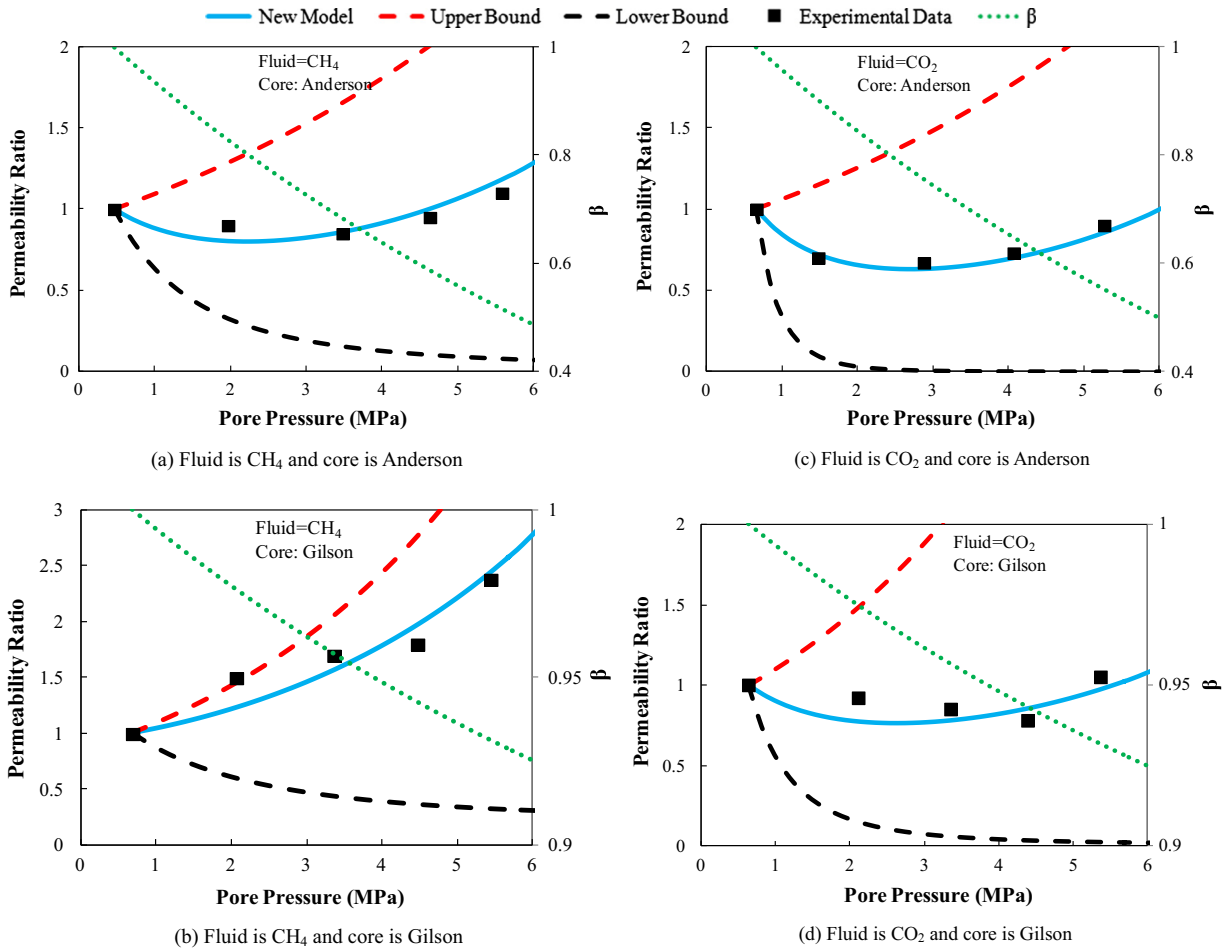


Fig. 10. Comparison of new model with experimental data obtained by Robertson and Christiansen [35], evolution of β and envelope of coal permeability evolution.

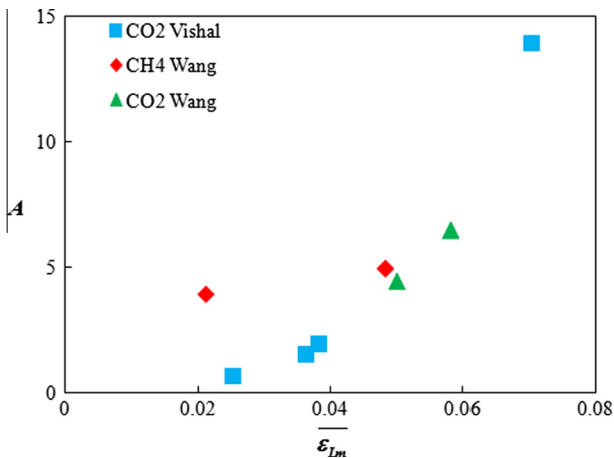


Fig. 11. Illustration of relationship of A with $\overline{\epsilon_{lm}}$.

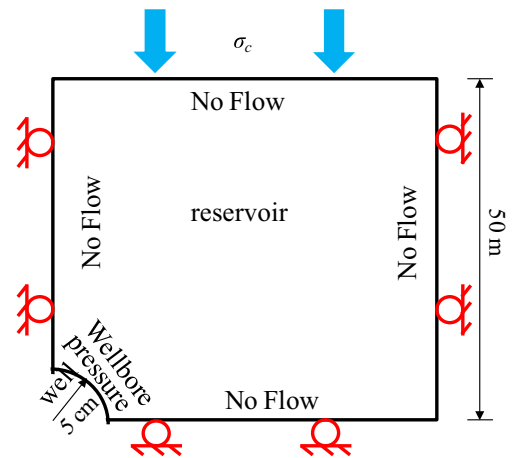


Fig. 12. Numerical model geometry and boundary conditions.

tions of the coal seam reservoir are: (1) uniaxial strain; (2) constant overburden stress at the top boundary; (3) the wellbore pressure is applied at the boundary of well; (4) no flow condition is applied at other boundaries. Values of parameters are collected from other studies [20,21,27,28] and list in Table 10.

5.5. Simulation results

To illustrate the impact of internal swelling strain on coal seam gas production, permeability models for two extreme cases: the

free swelling case and the constant volume case, are used to compare with the new permeability model. The model of free swelling case (Eq. (33)) ignores the impact of adsorption-induced strain on permeability evolution. Whereas, the model of constant volume case (Eq. (35)) assumes that the β_p is always 1 which overestimates the impact of internal swelling strain.

Fig. 13 shows the comparison of permeability evolution at a point between different cases. For the free swelling case, the permeability ratio always decreases due to the decrease of pore

Table 8
Langmuir constants for adsorption-induced strain curves for Anderson and Gilson coal at 80 °F [35].

Gas	Coal	ϵ_L	$\bar{\epsilon}_{Lm}$	A	Average P_L , MPa
CO ₂	Anderson	0.03527	0.013	2	3.83
	Gilson	0.01559	0.0085	0.3	
CH ₄	Anderson	0.00931	0.011	2	6.11
	Gilson	0.00765	0.003	0.3	

Table 9
Parameters used in matching the permeability obtained by Robertson and Christiansen [35].

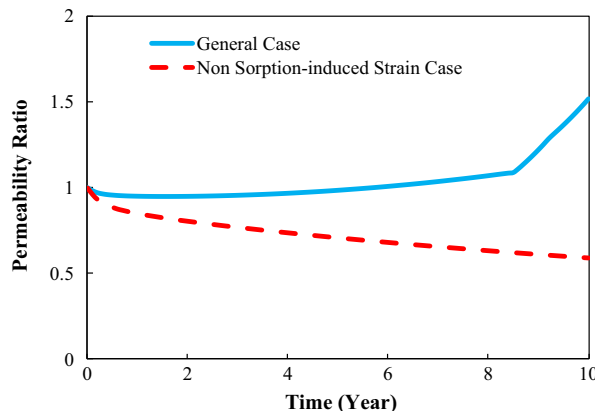
Symbol	Value	Units
μ_{CO_2}	1.5×10^{-5}	Pa s
μ_{CH_4}	1.2×10^{-5}	Pa s
ϕ_{0A}	1.31	%
P_0	6.89 ^a	MPa
E	1.4	GPa
c_{fA}	0.06 ^b	MPa ⁻¹
ν	0.35	-
ϕ_{0G}	0.804	%
c_{fG}	0.096 ^c	MPa ⁻¹
PC	16	MPa

^a It is 100 in unit of psi⁻¹.
^b It is 4.17×10^{-4} in unit of psi⁻¹.
^c It is 6.59×10^{-4} in unit of psi⁻¹.

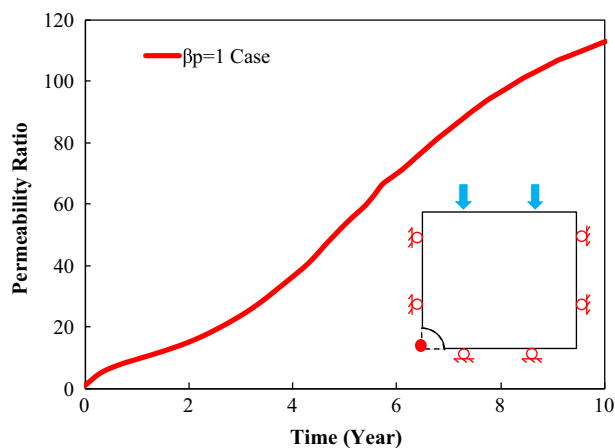
Table 10
Parameters used in numerical simulation.

Symbol	Value	Units
E	1.3	GPa
ν	0.3	-
α	0.6	-
ϕ_0	0.5	%
k_0	1.7×10^{-19}	m ²
P_0	10	MPa
P_L	6	MPa
$\bar{\epsilon}_L$	0.01	-
$\bar{\epsilon}_{Lm}$	0.025	-
V_L	0.01316	m ³ /kg
P_a	0.1	MPa
ρ_c	1500	kg/m ³
P_w	3	MPa
A	6	-
P_{Low}	2	MPa
σ_c	7	MPa
P_c	16	MPa

pressure during the gas depletion. For the constant volume case, the permeability ratio always increases due to the decrease of adsorption-induced strain during the gas depletion. If the proper characteristics of internal swelling strain are considered, the permeability ratio of the general case will be significantly different from those two cases: decreases at first and then increases. The permeability evolution depends on the evolution of β_p as shown in Fig. 14. The whole profile can be divided into two groups: zero and non-zero. When β_p is zero, the impact of internal swelling strain on permeability is not triggered and permeability evolution is determined by the effective stress. In this case, the permeability ratio slightly decreases and then increases. When β_p is non-zero, the impact of internal swelling strain on permeability is triggered. In this case, the permeability ratio significantly increases. Because of the obvious difference of permeability evolution between different cases, the recovery rates of different cases vary significantly as shown in Fig. 15.



(a) Evolutions of permeability ratio for general case and free swelling case



(b) Evolution of permeability ratio for constant volume case

Fig. 13. Illustration of evolutions of permeability ratio for different cases at a certain point (the coordinate of this point is (8,8), the origin of coordinates shows as the red dot). (For interpretation of the references to color in this figure legend, the reader is referred to the web version of this article.)

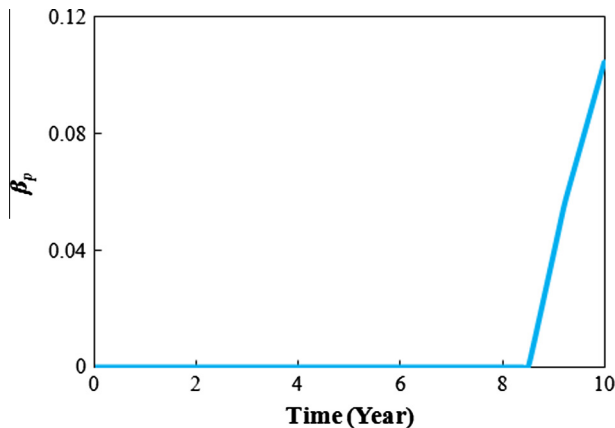


Fig. 14. Illustration of evolution of β_p at a certain point (the coordinate of this point is (8,8)).

Through this numerical simulation example, it shows that the new permeability model proposed in this study can be appropriately used in numerical simulation on coal seam gas production. These numerical results also show that the evolution of internal swelling strain plays a significant role in coal seam gas production.

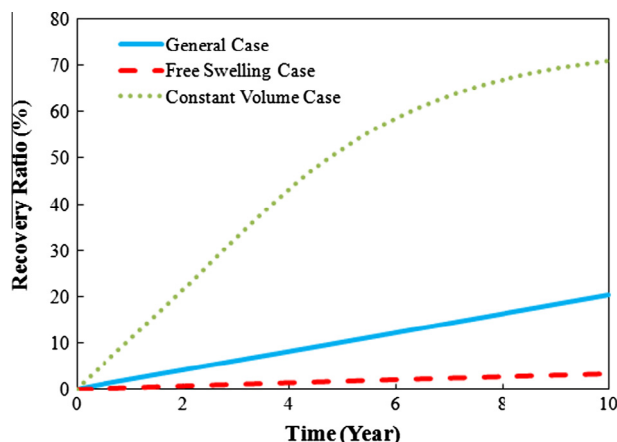


Fig. 15. Comparison of recovery rates between different cases.

6. Conclusions

In laboratory, the condition of constant confining pressure is commonly applied to coal samples. The permeability of those coal samples usually decreases first and then increases with increase of pore pressure. This phenomenon is difficult to be explained by current permeability models. In this study, based on the poroelasticity theory, the coal permeability with the effects of internal swelling strain, effective stress and gas adsorption-induced strain was proposed. The main difference between this new permeability model and other popular models is that this model considers the effect of internal swelling strain on permeability evolution. This improvement highly increases the accuracy of coal permeability model. This may also prove that the internal swelling strain is an important factor controlling the evolution of coal permeability under condition of constant confining pressure. In addition, the internal swelling strain results from the adsorption-induced swelling of matrix around fractures. The magnitude of the effect of internal swelling strain on permeability depends on (1) adsorption-induced swelling strain of matrix and (2) the heterogeneous distribution of internal swelling strain inside coal. Model results also show that the effect of internal swelling strain on permeability decreases as the swelling capacity of matrix increases. Although this new permeability model introduces the effect of internal swelling strain, it could be appropriately applied to the numerical simulation on coal seam methane production.

Acknowledgements

This work is partially funded by the National Natural Science Foundation of China (51474204 and 51604286), Science Foundation of China University of Petroleum, Beijing (Nos. 2462016YJRC034 and 2462014YJRC015), State Key Laboratory of Geomechanics and Geotechnical Engineering, Institute of Rock and Soil Mechanics, Chinese Academy of Sciences (No. Z014006), State Key Laboratory of Coal Resources and Safe Mining (China University of Mining and Technology) (No. SKLGRSM14KFB09), new staff start-up from the University of Queensland, UWA-UQ Bilateral Research Collaboration Award (2013002812), and ARC Discovery Project (DP150103467). These supports were gratefully acknowledged.

References

- [1] Seidle JR, Huitt L. Experimental measurement of coal matrix shrinkage due to gas desorption and implications for cleat permeability increases. In:

- Proceedings International meeting on petroleum Engineering 1995, Society of Petroleum Engineers; 1995.
- [2] Palmer I, Mansoori J. How permeability depends on stress and pore pressure in coalbeds: a new model. In: SPE Annual Technical Conference and Exhibition; 1996.
- [3] Harpalani S, Schraufnagel RA. Shrinkage of coal matrix with release of gas and its impact on permeability of coal. *Fuel* 1990;69:551–6.
- [4] Shi J-Q, Durucan S. A model for changes in coalbed permeability during primary and enhanced methane recovery. *SPE Reserv Eval Eng* 2005;8:291–9.
- [5] Connell L. Coupled flow and geomechanical processes during gas production from coal seams. *Int J Coal Geol* 2009;79:18–28.
- [6] Pan Z, Connell LD. Modelling permeability for coal reservoirs: a review of analytical models and testing data. *Int J Coal Geol* 2012;92:1–44.
- [7] Somerton WH, Söylemezoglu I, Dudley R. Effect of stress on permeability of coal. *Proc Int J Rock Mech Mining Sci Geomech Abstracts* 1975;12:129–45.
- [8] Schwere F, Pavone A. Effect of pressure-dependent permeability on well-test analyses and long-term production of methane from coal seams. In: SPE Unconventional Gas Recovery Symposium; 1984.
- [9] Pan Z, Connell LD. A theoretical model for gas adsorption-induced coal swelling. *Int J Coal Geol* 2007;69:243–52.
- [10] Gray I. Reservoir Engineering in Coal Seams Part 1-The Physical Process of Gas Storage and Movement in Coal Seams; 1987.
- [11] Gilman A, Beckie R. Flow of coal-bed methane to a gallery. *Transp Porous Media* 2000;41:1–16.
- [12] Shi J-Q, Pan Z, Durucan D. Analytical models for coal permeability changes during coalbed methane recovery: model comparison and performance evaluation. *Int J Coal Geol* 2014;136:17–24.
- [13] Palmer I. Permeability changes in coal: analytical modeling. *Int J Coal Geol* 2009;77:119–26.
- [14] Cui X, Bustin RM. Volumetric strain associated with methane desorption and its impact on coalbed gas production from deep coal seams. *AAPG Bull* 2005;89:1181–202.
- [15] Pekot L, Reeves S. Modeling coal matrix shrinkage and differential swelling with CO₂ injection for enhanced coalbed methane recovery and carbon sequestration applications. Topical Report, Contract No. DE-FC26-00NT40924, US DOE, Washington, DC (November 2002); 2002.
- [16] Robertson E, Christiansen R. A permeability model for coal and other fractured, sorptive-elastic media. SPE Eastern Regional Meeting 2006.
- [17] Zhang H, Liu J, Elsworth D. How sorption-induced matrix deformation affects gas flow in coal seams: a new FE model. *Int J Rock Mech Min Sci* 2008;45:1226–36.
- [18] Liu J, Chen Z, Elsworth D, Qu H, Chen D. Interactions of multiple processes during CBM extraction: a critical review. *Int J Coal Geol* 2011;87:175–89.
- [19] Robertson E, Christiansen RL. Modeling permeability in coal using sorption-induced strain data. In: SPE Annual Technical Conference and Exhibition; 2005.
- [20] Pini R, Ottiger S, Burlini L, Storti G, Mazzotti M. Role of adsorption and swelling on the dynamics of gas injection in coal. *J Geophys Res: Solid Earth* 2009;114:1078–2012:114.
- [21] Wang S, Elsworth D, Liu J. Permeability evolution in fractured coal: the roles of fracture geometry and water-content. *Int J Coal Geol* 2011;87:13–25.
- [22] Vishal V, Ranjith P, Pradhan S, Singh T. Permeability of sub-critical carbon dioxide in naturally fractured Indian bituminous coal at a range of down-hole stress conditions. *Eng Geol* 2013;167:148–56.
- [23] Shi J-Q, Durucan D, Shimada S. How gas adsorption and swelling affects permeability of coal: a new modelling approach for analysing laboratory test data. *Int J Coal Geol* 2014;128–129:134–42.
- [24] Liu H-H, Rutqvist J. A new coal-permeability model: internal swelling stress and fracture-matrix interaction. *Transp Porous Media* 2010;82:157–71.
- [25] Connell LD, Lu M, Pan Z. An analytical coal permeability model for tri-axial strain and stress conditions. *Int J Coal Geol* 2010;84:103–14.
- [26] Chen Z, Liu J, Pan Z, Connell LD, Elsworth D. Influence of the effective stress coefficient and sorption-induced strain on the evolution of coal permeability: model development and analysis. *Int J Greenhouse Gas Control* 2012;8:101–10.
- [27] Liu J, Wang J, Chen Z, Wang S, Elsworth D, Jiang Y. Impact of transition from local swelling to macro swelling on the evolution of coal permeability. *Int J Coal Geol* 2011;88:31–40.
- [28] Qu H, Liu J, Pan Z, Connell L. Impact of matrix swelling area propagation on the evolution of coal permeability under coupled multiple processes. *J Nat Gas Sci Eng* 2014;18:451–66.
- [29] Peng Y, Liu J, Zhu W, Pan Z, Connell L. Benchmark assessment of coal permeability models on the accuracy of permeability prediction. *Fuel* 2014;132:194–203.
- [30] Izadi G, Wang S, Elsworth D, Liu J, Wu Y, Pone D. Permeability evolution of fluid-infiltrated coal containing discrete fractures. *Int J Coal Geol* 2011;85:202–11.
- [31] Zhu W, Wei C, Liu J, Xu T, Elsworth D. Impact of gas adsorption induced coal matrix damage on the evolution of coal permeability. *Rock Mech Rock Eng* 2013;46:1353–66.
- [32] Peng Y, Liu J, Wei M, Pan Z, Connell L. Why coal permeability changes under free swellings: new insights. *Int J Coal Geol* 2014.
- [33] Karacan CÖ. Swelling-induced volumetric strains internal to a stressed coal associated with CO₂ sorption. *Int J Coal Geol* 2007;72:209–20.
- [34] Mao L, Hao N, An L, Chiang F-P, Liu H. 3D mapping of carbon dioxide-induced strain in coal using digital volumetric speckle photography technique and X-ray computer tomography. *Int J Coal Geol* 2015;147:115–25.

- [35] Robertson EP, Christiansen RL. Modeling laboratory permeability in coal using sorption-induced strain data. *SPE Reserv Eval Eng* 2007;10(3):260–9.
- [36] Crosdale PJ, Beamish B, Valix M. Coalbed methane sorption related to coal composition. *Int J Coal Geol* 1998;35:147–58.
- [37] Karacan C, Okandan E. Adsorption and gas transport in coal microstructure: investigation and evaluation by quantitative X-ray CT imaging. *Fuel* 2001;80:509–20.
- [38] Karacan CÖ. Heterogeneous sorption and swelling in a confined and stressed coal during CO₂ injection. *Energy Fuels* 2003;17:1595–608.
- [39] Pan Z, Connell LD, Camilleri M, Connelly L. Effects of matrix moisture on gas diffusion and flow in coal. *Fuel* 2010;89:3207–17.
- [40] Zheng G, Pan Z, Tang S, Ling B, Lv D, Connell LD. Laboratory and modeling study on gas diffusion with pore structures in different-rank Chinese coals. *Energy Explor Exploit* 2013;31:859–78.
- [41] Shi J-Q, Durucan S. Modelling laboratory horizontal stress and coal permeability data using S&D permeability model. *Int J Coal Geol* 2014;131:172–6.